National Research Council Canada
Conseil national de recherches Canada
Institute for Aerospace Research
Institut de recherche aérospatiale

Unclassified/Proprietary Limited

NRC·CNRC

Frangibility Analysis of Approaching Lighting Composite Tower

LTR-SMPL-2009-0120

M. Nejad Ensan

July 2009

Canada

INSTITUTE FOR AEROSPACE RESEARCH

REPORT
RAPPORT

INSTITUT DE RECHERCHE AÉROSPATIALE

Pages: 36

Tables: 2

Figures: 13

STRUCTURES AND MATERIALS PERFORMANCE LABORATORY

LABORATOIRE DE PERFORMANCE DES STRUCTURES ET DES MATÉRIAUX

Report No.: LTR-SMPL-2009-0120

Date: 27-July-2009

Classification: Unclassified/Proprietary
Distribution: Limited

For:
Pour: Exel Composites Oyj
Muovilaaksontie 2
FI-82110 Heinävaara, Finland

Reference:
Référence:

LTR-SMPL-2009-0120

Frangibility Analysis of Approach Lighting Composite Tower

Submitted by:
Présenté par: P. Patnaik
Director/Directeur

Author(s):
Auteur(s): M. Nejad Ensan

Approved by:
Approuvé par: J. Komorowski
Director General/Directeur général

Table of Content

1 Introduction

Airport approach lighting towers are used at airports to aid in visual navigation of aircraft. The close proximity of these towers to the runways requires that the towers be designed to cause minimal damage, if any, to aircraft in case of a collision between the pole and the aircraft. Full-scale impact tests are generally used to assess compliance with certification requirements such as "Aerodrome Design Manual, Part 6, Frangibility" [1] or the Advisory Circular (AC) No. 150/5345-45C of Federal Aviation Administration (FAA) [2].

2 Report Outline

This report describes the full-scale impact test on the representative airport approach lighting pole D106 and lattice tower L500 of Exel Composite Oyj. This report also describes the approach taken for the impact test which includes the tower configuration, test instrumentation, data analysis and test procedures used to perform the impact test. The report includes the results of the impact tests, which consist of failure mode, impact force and impact energy during several impact test configurations.

3 Full-scale Test

Full-scale impact tests on the Exel Composite Oyj representative airport lighting pole D106 and lattice tower L500 were carried out at the "Research and Test Centre" in Blainville, Quebec, Canada by PMG Technologies Inc. IAR/NRC developed the test procedure, conducted data analysis and coordinated the test program with the PMG test facility. The objective of the test was to investigate the key parameters including the maximum force developed and the energy absorbed during the impact, as well as the failure mode and compare these to recommended values proposed by AC No. 150/5345-45C of FAA.

3.1 General Setup

The general test configuration is presented in Figure 1. The pole and lattice tower were mounted in a pit on the side of a test track with the base of the pole/lattice tower bolted to a base-plate fixed in a concrete foundation as shown in Figure 2. The rigid impactor was mounted on a truck (Figure 3) such that the point of impact was one meter (3.28') down from the top of the tower. The impact velocity was controlled through the cruise control mechanism of the truck and the speed was recorded before, during and after the impact on the data acquisition system using an Oxford GPS speed sensor model RT3002. One data acquisition system located in the truck was used for recording impact force measurement on the tower. Three high-speed video cameras and a still camera were used to record the events of the impact. On initiation of the impact, a trigger strip on the impactor provided a signal for the video recording and data acquisition system to mark the beginning of the impact. A second trigger strip was mounted on the test specimen to mark the beginning of impact for the non-onboard cameras.

3.2 Test Structures

3.2.1 D106 Airport approach lighting pole

The D106 pole structure used for the tests consisted of three sections totaling 4.6m (15.1ft) in height as shown in Figure 4. The top section was attached through a middle section to the bottom section. All sections had a circular cross-section with the top section having a diameter of 51mm (2in), the middle section having a diameter of 86 mm (3.4in) and the bottom section having a diameter of 106mm (4.2in). The wall thicknesses of the pole sections were 2.5mm, 2.0mm and 3.0mm (0.098in, 0.079in, 0.118in) from top to bottom and they were joined together with aluminum bushings bonded to the tube. The tube sections were made of fiber glass composite material with minimum yield strength of 285 MPa (41,340 psi). A top mass of 2.0 kg (4.4 lbs) was added to the pole to represent the approach light and fixtures. This top mass was made in the shape of a cylindrical weight, which was bolted to the top of the pole. The pole was tested with an electrical cable installed.

3.2.2 L500 Airport approach lighting lattice tower

The L500 lattice structure used for the tests consisted of two lattice sections totaling 6.1m (20ft) in length as shown in Figure 5. The top section was attached through a square cross section plate to the bottom section. The top section had a square cross-section of 400×400 mm (15.75in×15.75in) and a height of 5.25m (17.22ft). The vertical rods of the top section were 32mm (1.26in) in diameter and the diagonal tie rods were made of 22mm (0.87in) diameter fiber glass composite material with minimum yield strength of 285 MPa (41,340 psi). The bottom section had a square cross-section of 500×500 mm (19.69in ×19.69in) and a height of 0.67m (2.2in). The vertical rods of the bottom section were 51mm (2in) in diameter and the diagonal tie rods made of 32mm (1.26in) diameter fiber glass composite material with minimum yield strength of 285 MPa (4,1340 psi). A top mass of 26 kg (57.3 lbs) was added to the tower to represent approach lights and fixtures. This top mass was made in the shape of two cylindrical weights, which were bolted to the top of the tower. The tower was tested with electrical cables installed, which were attached to the tower through two cylindrical tubes. The tower was tested in two orientations; one with both cylindrical cable tubes facing the impactor, and the other with both cylindrical cable tubes on the opposite side of the impactor.

3.3 Impactor

The rigid impactor was built based on the requirement of AC 150/5345-45C of FAA section 4.2.5.1 of “Test Instrumentation and Procedure”, and was accepted by the FAA test inspector. The impactor was a rigid semicircular mild steel tube 0.79m long. The outer diameter of the tube was 250 mm with a wall thickness of 22.9 mm. The impactor was mounted on the support structure attached to the test vehicle as shown in Figure 3. An aluminum plate was attached to the rigid impactor and another was attached to the support structure. Three compression load cells were mounted between these plates to measure the impact force. A thin steel covering plate was placed over the two thick plates carrying the load cells to prevent the approach lighting structure from catching on the plates during the impact. This plate covered the support structure behind the impactor, to reduce the possibility of the approach lighting structure interacting with the supporting structure as a result of the additional deflection expected due to the top mass.

3.4 Instrumentation Overview

A description of the instrumentation used during the impact test program is provided below. More information is given in Appendix A. Instrumentation was provided by PMG Technologies to measure the following parameters:

3.4.1 Impact force

Three 10 000 pounds force compression load cells were used to measure the impact force. The load cells were attached between two aluminum plates. The first plate was attached to the impactor and the second plate was fixed to the support structure. The total impact force was determined as the sum of the recorded data from the load cells.

3.4.2 Velocity

The driver of the truck used the cruise control system of the vehicle to stabilize the speed of the truck at the required value (140 km/h) before the impact. In addition, the truck speed was measured at the moment of impact for each test by an Oxford GPS speed sensor model RT3002.

3.4.3 Data acquisition system

The impact force on the three load cells and speed of truck were recorded by an Astromed System, model Dash 18. The data acquisition system was set to a recording rate of 10 kHz. The data recorder was located in the truck cab.

3.4.4 Calibration of the measurement equipment

All instrumentations used in the test were within calibration. See Appendix A for more details on project instrumentation and calibration documents.

3.4.5 Photographic, video and film camera coverage

Digital and regular cameras were used for documentation of the tests. Two video cameras were used to provide a general view of the test sequence. Three high-speed video cameras and one high speed still camera were used to record the impact sequence, to capture the mode of failure. The high-speed video cameras were capable of recording 2000 frames/second. The output from the videos has been copied and assembled on a DVD for documentation purpose (see Appendix B). All pictures in this report were taken by the camera noted above.

A summary of equipment and instrumentation are presented in Table 1.

Table 1: Summary of equipment and instrumentation

Description	Manufacturer	Model	Serial	Calibration date
Data acquisition system	Astromed Dash 18x	Dash 18x	08B0246	March 11th, 2009
GPS speed sensor	Oxford	RT3002	354	February, 2nd, 2008 (Required calibration cycle is every two years)
Load cell 1	Eaton	3157-101	1872a	April 29th, 2009
Load cell 2	Eaton	3157-101	1874a	April 29th, 2009
Load cell 3	Eaton	3157-101	1903a	April 29th, 2009

4 Test Results

For each test, the impact force and energy were obtained or calculated from recorded data. Energy was calculated by numerical integration of the recorded impact force with respect to distance using the following equation:

$$E = \int_0^x F\,dx = v\int_0^t F\,dt \qquad \text{(Eq. 1)}$$

Where E is the energy, F is the measured force, v is the velocity and t represents the time. In deriving the above equation, the velocity of the impactor was assumed to be constant during the very short impact, which was shown to be a good approximation from the data.

4.1 Impact Test of D106 Pole

The pole was mounted in a pit on the side of a test track and the pole base-plate fixture was bolted to a concrete foundation. The impactor, which was mounted on a truck such that the impact point was one meter down from the top of the pole, struck the pole at a high impact speed of around 142 km/h. The speed-time curve is shown in Fig. 6. It can be observed that the speed of the truck was almost constant during the impact event. The pole contained a dummy top mass of 2.0 kg (4.4 lbs) representative of light fixtures and lights. The impact events were analyzed for a time period of 0.1 s, which was chosen to be sufficiently long to analyze the initial events of the impact. Dynamic results were recorded at one thousand equal time steps (every 0.0001 s).

4.1.1 Deformation and failure mode

Test image frames from the full-scale test for this impact case are shown in Fig. 7. The time resolution of the video image was 0.5 millisecond (ms). The test image frames showed that the top portion of the pole separated from the bottom portion. This top portion wrapped around the impactor for the first 82 ms and was then dropped. A failure mode of fracturing combined with bending was observed. The average time to failure was 3 ms. It should be noted that the energy to failure was not as significant as the energy transferred during the contact period. After failure, the pole remained in contact with the impactor for 82 ms and energy was still being transferred to the impactor. In addition; the electrical cabling separated and did not impede the fracturing or bending of the structure. The impactor did not become entangled with cabling.

4.1.2 Impact force

The magnitude of the impact force versus time is represented in Fig. 8. It can be observed that the first maximum load represented the first peak load (12.3 kN) experienced by the pole, occurred during the first 4 ms after impact. It is believed that the oscillations in the full-scale test impact force-time curve were a result of vibration in the impactor and/or impactor support structure.

4.1.3 Energy absorption

The energy absorption curve versus time obtained from the full-scale test is shown in Fig 9. Kinetic energy was imparted to the pole during the contact period between the pole and impactor and remained with the pole throughout the impact. The maximum final energy level was 5.3 kJ. It would appear that the calculated values for energy approached a maximum value asymptotically.

4.2 Impact Test of L500 Lattice Tower

The L500 Lattice Tower was mounted in a pit on the side of a test track and the tower base-plate fixture was bolted to a concrete foundation. The impactor which was mounted on a truck such that the impact point was one meter down from the top of the tower struck the tower at a high impact speed of around 142 km/h. The speed-time curve is shown in Fig. 10.a-b. It can be observed that the speed of the truck was almost constant during the impact event. Impact tests of the L500 Lattice Tower were performed under two scenarios with:

a) the electrical cables run on the impactor side and
b) the electrical cables run opposite to the impactor side

The tower contained a dummy top mass of 26 kg (57.3 lbs) representative of light fixtures and lights. The impact events were analyzed for a time period of 0.1 s, which was chosen to be sufficiently long to analyze the initial impact events. Dynamic results were recorded at one thousand equal time steps (every 0.0001 s).

4.2.1 Deformation and failure mode

Test image frames from the full-scale test for the impact scenarios (a) and (b) are shown in Fig. 11.a-b, respectively. The time resolution of the video image was 0.5 millisecond (ms). The average time to failure was approximately 2 ms. The test image frames showed that the tower wrapped around the impactor for approximately 25 ms. Then the tower shattered into many lightweight pieces. It should be noted that the energy to failure was not as significant as the energy transferred during the contact period. After failure, the tower remained in contact with the impactor for 78 ms for scenario (a) and energy was still being transferred to the impactor.

In addition; electrical cabling separated and did not impede the failure or bending of the tower.

4.2.2 Impact force

The magnitude of the impact force versus time for two scenarios (a) and (b) are shown in Fig. 12.a-b, respectively. It can be observed that the first maximum load represented the first peak load (37.4 and 36.0 kN for scenario (a) and (b), respectively) experienced by the tower occurred during the first 4 ms after impact. It is believed that the oscillations in the full-scale test impact force-time curve were a result of vibration in the impactor and/or impactor support structure.

Fig. 12b showed two peaks that were significant both in terms of their magnitude and the time at which they occurred. The first of these peaks occurred during the first 4 ms after impact with a magnitude of 36.0 kN. The second peak occurred during the latter stage of the impact after 30 ms with a magnitude of 38.3 kN. This second peak may be attributed to the electrical cabling position in scenario (b).

4.2.3 Energy absorption

The energy absorption curve versus time obtained from full-scale test is shown in Fig 13.a-b. Kinetic energy was imparted to the pole during the contact period between the pole and impactor and remained with the pole throughout the impact. The maximum final energy level was 32.1 and 26.8 kJ. It would appear that the calculated values for energy approached a maximum value asymptotically.

5 Comparison with AC No. 150/5345-45C of FAA Recommendation

Section 4.2.5.2 of AC 150/5345-45C of FAA on Low-Impact Resistant (LIR) Structure on “Acceptance/rejection Criteria” states that:

a. The LIR structure must not impose a force of greater than 10,116 lbs force (45 kN) peak on the impactor per recordings from the load cells. The maximum energy imparted to the impactor by the structure must not exceed 40,566 ft-lbs (55 kJ) peak during structure contact time.

b. View the high speed video or film recording, verify that the structure does not remain anchored to its foundation and could potentially grasp the wing of the aircraft so that the direction of the aircraft would be adversely affected.

c. The failure mode of the structure must be: fracturing, windowing, or bending.

d. A structure section that wraps around the impactor must not be considered a failure if the section separates from the structure (structure fragments) or the bottom portion of the structure separates from the foundation.

e. Electrical cabling must separate and not impede the fracturing, windowing, or bending of the structure. If the impactor becomes entangled with electrical cabling or structure sections that are held together by the cabling, determine if this would hinder the continued flight and safe operation of an aircraft the size of a Piper Aztec or similar aircraft (approximately 6600 lbs (3000 kg)).

f. Structure fragments after impact should not be of a sufficient mass to cause severe damage to an aircraft (punch a hole through the fuselage, tail surfaces, shatter windows or a wind screen).

g. In lieu of the testing detailed in this section, products that already qualify to the requirements of FAA-E-2702 and FAA Drawings D-6155-1 through 46 are considered as meeting the requirements of this AC.

A summary comparison of obtained test results with AC No. 150/5345-45C of FAA requirements is presented in Table 2. In this Table actual speeds measured just before impact are included in the first row. The maximum impact force shown was obtained from the load cell measurements. The value for impact energy shown in the table was obtained using equation 1 (Eq. 1) by integrating the force over the contact period. In computing the energy terms using equation 1 (Eq. 1), the velocity measured just before the impact was used.

All the results from testing met the maximum energy requirement of 55 kJ. In addition, the maximum force requirement was met by all of the results.

Table 2: Summary comparison of obtained test results with AC No. 150/5345-45C of FAA Requirements

Requirement	Actual value D106	Actual value L500, wires on impactor side	Actual value L500, wires opposite of impactor side
a. The LIR structure must not impose a force of greater than 10,116 lbs force (45 kilo Newtons) peak on the impactor per recordings from the load cells. The maximum energy imparted to the impactor by the structure must not exceed 40,566 ft. lbs. (55 kJ) peak during structure contact time.	Impact speed: 142.8 km/h Maximum force: 12.2 kN Energy: 5.3 kJ	Impact speed: 142.7 km/h Maximum force: 37.4 kN Energy: 32.1 kJ	Impact speed: 142.3 km/h Maximum force: 38.3 kN Energy: 26.8 kJ
b. View the high speed video or film recording, verify that the structure does not remain anchored to its foundation and could potentially grasp the wing of the aircraft so that the direction of the aircraft would be adversely affected.	Top section of the pole separated from the bottom section. The structure lightly wrapped around the impactor. Please see the attached DVD for more detail.	Structure does remain anchored to its foundation. The structure lightly wrapped around the impactor. Please see the attached DVD for more detail.	Structure does remain anchored to its foundation. The structure lightly wrapped around the impactor. Please see the attached DVD for more detail.
c. The failure mode of the structure must be: fracturing, windowing, or bending.	Failure mode is fracturing combined to bending. Please see the attached DVD for more detail.	Failure mode is fracturing combined to bending. Please see the attached DVD for more detail.	Failure mode is fracturing combined to bending. Please see the attached DVD for more detail.
d. A structure section that wraps around the impactor must not be considered a failure if the section separates from the structure (structure fragments) or the bottom portion of the structure separates from the foundation.	The structure lightly wrapped around the impactor for a period of 82 ms. The top section of the structure separated from the bottom section. Please see the attached DVD for more detail.	The structure lightly wrapped around the impactor for a period of 78 ms. The structure collapsed on the ground and was no longer attached to the foundation. Please see the attached DVD for more detail.	The structure lightly wrapped around the impactor for a period of 90 ms. The structure collapsed on the ground and was no longer attached to the foundation. Please see the attached DVD for more detail.
e. Electrical cabling must separate and not impede the fracturing, windowing, or bending of the structure. If the impactor becomes entangled with electrical cabling or structure sections that are held together by the cabling, determine if this would hinder the continued flight and safe operation of an aircraft the size of a Piper Aztec or similar aircraft (approximately 6600 lbs (3000 kg)).	Electrical cabling separated and did not impede the fracturing or bending of the structure. Impactor did not become entangled with cabling. Please see the attached DVD for more detail. The investigation on whether the impact would hinder the continued flight and safe operation of an aircraft the size of a Piper Aztec or similar aircraft (approximately 6600 lbs (3000 kg)) was not performed.	Electrical cabling separated and did not impede the fracturing or bending of the structure. Impactor did not become entangled with cabling. Please see the attached DVD for more detail. The investigation on whether the impact would hinder the continued flight and safe operation of an aircraft the size of a Piper Aztec or similar aircraft (approximately 6600 lbs (3000 kg)) was not performed.	Electrical cabling separated and did not impede the fracturing or bending of the structure. Impactor did not become entangled with cabling. Please see the attached DVD for more detail. The investigation on whether the impact would hinder the continued flight and safe operation of an aircraft the size of a Piper Aztec or similar aircraft (approximately 6600 lbs (3000 kg)) was not performed.
f. Structure fragments after impact should not be of a sufficient mass to cause severe damage to an aircraft (punch a hole through the fuselage, tail surfaces, shatter windows or a wind screen).	Structure fragments after impact were lightweight. Please see the attached DVD for more detail.	Structure fragments after impact were lightweight. Please see the attached DVD for more detail.	Structure fragments after impact were lightweight. Please see the attached DVD for more detail.
g. In lieu of the testing detailed in this section, products that already qualify to the requirements of FAA-E-2702 and FAA Drawings D-6155-1 through 46 are considered as meeting the requirements of this AC.	Not applicable	Not applicable	Not applicable

6 Conclusions

Exel Composite Oyj. is in the process of certifying the frangibility of the D106 pole and L500 lattice tower based on the AC 150/5345-45C of FAA. The frangibility tests of these structures were performed at the “Research and Test Centre” in Blainville, Quebec, Canada by PMG Technologies Inc. IAR/NRC developed the test procedure, conducted data analysis and coordinated the test program with the PMG test facility. These tests took place from May 19 to May 21, 2009.

A series of full-scale impact tests simulating the transient dynamic impact resulting from a collision between an aircraft and approach lighting D106 pole and L500 tower has been completed and presented in this report.

The results obtained from impact tests of the Exel Composite Oyj D106 approach lighting pole and L500 tower met the maximum energy requirement of 55 kJ. In addition, the maximum force requirement was met by all of the results.

7 Acknowledgements

The author would like to acknowledge invaluable contribution from C. Sauvageau and his team from the PMG Technologies Inc, as well as Jaakko Martikainen from Exel Composites Oyj in performing the impact tests of the approach lighting pole and tower.

8 References

1. International Civil Aviation Organization, “Aerodrome Design Manual, Part 6, Frangibility, First Edition, 2006.
2. Advisory Circular No. 150/5345-45C of Federal Aviation Administration on Low-Impact Resistant Structure, April 2007.

Appendix A

Technical Information and Calibration Certification of the Test Equipment

Astro-Med, Inc
Astro-Med Industrial Park, 600 East Greenwich Avenue
West Warwick, RI 02893 • 401-828-4000 • FAX 401-822-2430

Repair Report/Calibration Certificate

Customer Name: ASTRO MED CDA

Model: DASH 18X

Serial Number: 08B0246

Return Material Authorization (RMA): 59155

Reported Problem: WON'T BOOT INTO WINDOWS

Received in tolerance _______ **out of tolerance** _X__
Returned in tolerance __X___ **out of tolerance** ____

Actual problems found: WON'T BOOT INTO WINDOWS, BROKEN CLIPS FOR STAND, DISPLAY BRACKET NEEDED

Corrective action: REPLACED HARD DRIVE, CLIPS AND DISPLAY BRACKET

Repaired by:D. RICCI

This is to certify that the instrument described above has been calibrated in accordance with the Original Manufacturer's established standards and procedures for original equipment performance. Calibration was performed with standard test equipment and laboratory standards traceable to the National Institute of Standards and Technology, and the instrument described has been found to meet or exceed the manufacturer's requirements for original instrument performance. The cycling and certification of all measurement standards used by Astro-Med,Inc. meet the requirements of MIL-STD-45662A and ANSI/NCSL Z540-1-1994.

Date Certified: 03/10/2009

Certified By: [signature]

Recertification: 03/10/2010

Temp: 70F
%rh: 45% +/- 15%

Standard	NIST Cert#
DC voltage	Josephson Array
AC voltage	257311
Resistance	259415
Frequency	VLF Transmission

DENTON

DENTON ATD, INC.

2967 Waterview Drive, Rochester Hills, MI 48309

Tel (248) 852-5100 - Fax (248) 852-6060 - email: info@radenton.com - www.radenton.com

Calibration Report

Bi-Directional Calibration (negative)

Automated Load Cell Calibration System

Calibration No.	A5293006G	Date	Apr 29, 2009	Due(4)	Apr 29, 2010
Model No.	3157-101	Serial No.			1872A
Technician	J. Burchi	Temp (C) / Hum. (%)			24.1 / 35.3
Customer	PMG	Last Calibrated			Aug 12, 2008
Description	Load Cell	Customer Tag Number			N/A

Voltage Calibration

Bridge	Capacity	Zero Offset	Nonlinearity	Hysteresis	Output @ Capacity	% Change
Force	44482.2 N	-0.0028 mV/V	0.01 % FS	0.03 % FS	-2.9902 mV/V	0.00 % FS

Shunt

Bridge	Shunt Value	Equivalent Load	Bridge Resistance (nom)
Force	40.0 K Ohms	-32500.6 N	350.0 Ohms

NOTE: Positive shunt is between +Exc_+Sig Negative shunt is between -Exc_+Sig

Wire Color Codes

	Force		N/A		N/A
Pin A	+ Exc.	N/A	+ Exc.	N/A	+ Exc.
Pin B	+ Sig.	N/A	+ Sig.	N/A	+ Sig.
Pin D	- Exc.	N/A	- Exc.	N/A	- Exc.
Pin C	- Sig.	N/A	- Sig.	N/A	- Sig.

Reference Load Cell

Manufacturer	Model No.	Serial No.	Calibration Due Date
Interface	1110AO-10K	108177	Feb 2, 2010

Calibrated by ______________________

Robert A. Denton, Inc. Authorized Representative

DENTON ATD, INC.
2967 Waterview Drive, Rochester Hills, MI 48309
Tel (248) 852-5100 · Fax (248) 852-6860 · email: info@radenton.com · www.radenton.com

DENTON

Calibration Report
Bi-Directional Calibration (negative)

Automated Load Cell Calibration System

Calibration No.	A5293004G	Date Apr 29, 2009 Due(4)	Apr 29, 2010
Model No.	3157-101	Serial No.	1874A
Technician	J. Burchi	Temp (C) / Hum. (%)	24.0 / 34.6
Customer	PMG	Last Calibrated	Aug 12, 2008
Description	Load Cell	Customer Tag Number	N/A

Voltage Calibration

Bridge	Capacity	Zero Offset	Nonlinearity	Hysteresis	Output @ Capacity	%Change
Force	44482.2 N	0.0072 mV/V	0.01 % FS	0.02 % FS	-2.9923 mV/V	0.00 % FS

Shunt

Bridge	Shunt Value	Equivalent Load	Bridge Resistance (nom)
Force	40.0 K Ohms	-32527.5 N	350.0 Ohms

NOTE: Positive shunt is between +Exc_+Sig Negative shunt is between -Exc_+Sig

Wire Color Codes

	Force	N/A		N/A	
Pin A	+ Exc.	N/A	+ Exc.	N/A	+ Exc.
Pin B	+ Sig.	N/A	+ Sig.	N/A	+ Sig.
Pin D	- Exc.	N/A	- Exc.	N/A	- Exc.
Pin C	- Sig.	N/A	- Sig.	N/A	- Sig.

Reference Load Cell

Manufacturer	Model No.	Serial No.	Calibration Due Date
Interface	1110AO-10K	108177	Feb 2, 2010

Calibrated by ____________________ JK
Robert A. Denton, Inc. Authorized Representative

DENTON

DENTON ATD, INC.

2967 Waterview Drive, Rochester Hills, MI 48309

Tel (248) 852-5100 · Fax (248) 852-6060 · email: info@radenton.com · www.radenton.com

Calibration Report

Bi-Directional Calibration (negative)

Automated Load Cell Calibration System

Calibration No.	**A5293005G**	**Date** Apr 29, 2009 **Due(4)**	**Apr 29, 2010**
Model No.	**3157-101**	**Serial No.**	**1903A**
Technician	**J. Burchi**	**Temp (C) / Hum. (%)**	**24.0 / 34.6**
Customer	**PMG**	**Last Calibrated**	**Aug 12, 2008**
Description	**Load Cell**	**Customer Tag Number**	**N/A**

Voltage Calibration

Bridge	Capacity	Zero Offset	Nonlinearity	Hysteresis	Output @ Capacity	% Change
Force	44482.2 N	0.0641 mV/V	0.01 % FS	0.04 % FS	-2.9852 mV/V	0.00 % FS

Shunt

Bridge	Shunt Value	Equivalent Load	Bridge Resistance (nom)
Force	40.0 K Ohms	-32653.1 N	350.0 Ohms

NOTE: Positive shunt is between +Exc_+Sig Negative shunt is between -Exc_+Sig

Wire Color Codes

	Force		N/A		N/A
Pin A	+ Exc.	N/A	+ Exc.	N/A	+ Exc.
Pin B	+ Sig.	N/A	+ Sig.	N/A	+ Sig.
Pin D	- Exc.	N/A	- Exc.	N/A	- Exc.
Pin C	- Sig.	N/A	- Sig.	N/A	- Sig.

Reference Load Cell

Manufacturer	Model No.	Serial No.	Calibration Due Date
Interface	1110AO-10K	108177	Feb 2, 2010

Calibrated by ____________________

Robert A. Denton, Inc. Authorized Representative

Equipment under Calibration

Model:	RT3002	IMU Dev ID:	060616.14ab
Serial Number:	354	Cal ID:	"354_080226"

Test Equipment

Procedure:	14A0001I
Cal Software:	070702.14g

IMU Calibration Values

Measured Alignment Matrix and Bias Vector for the Accelerometers and Gyros are:

$$Ma = \begin{bmatrix} 0.999939 & 0 & 0 \\ -3.000466\cdot10^{-5} & 0.999927 & 0 \\ 1.176299\cdot10^{-5} & -6.332907\cdot10^{-6} & 0.999881 \end{bmatrix} \qquad Ba = \begin{bmatrix} 1.106\cdot10^{-4} \\ -7.223\cdot10^{-5} \\ -2.77\cdot10^{-4} \end{bmatrix}$$

$$Mg = \begin{bmatrix} 0.999918 & 5.486968\cdot10^{-5} & -9.602195\cdot10^{-5} \\ -4.115226\cdot10^{-5} & 0.999918 & 8.230453\cdot10^{-5} \\ 2.743484\cdot10^{-5} & -1.508916\cdot10^{-4} & 1 \end{bmatrix} \qquad Bg = \begin{bmatrix} -2.408\cdot10^{-3} \\ 5.044\cdot10^{-3} \\ 3.777\cdot10^{-3} \end{bmatrix}$$

Difference from ideal and limits:

$$AccMDiff = \begin{bmatrix} -6.071\cdot10^{-3} & 0 & 0 \\ -1.719\cdot10^{-3} & -7.339\cdot10^{-3} & 0 \\ 6.74\cdot10^{-4} & -3.628\cdot10^{-4} & -0.012 \end{bmatrix} \qquad AccMLimits := \begin{bmatrix} 0.05 & 0.01 & 0.01 \\ 0.01 & 0.05 & 0.01 \\ 0.01 & 0.01 & 0.05 \end{bmatrix}$$

$$AccBDiff = \begin{bmatrix} 1.106\cdot10^{-4} \\ -7.223\cdot10^{-5} \\ -2.77\cdot10^{-4} \end{bmatrix} \qquad AccBLimits := \begin{bmatrix} 0.01 \\ 0.01 \\ 0.01 \end{bmatrix}$$

$$GyroMDiff = \begin{bmatrix} -8.23\cdot10^{-3} & 3.144\cdot10^{-3} & -5.502\cdot10^{-3} \\ -2.358\cdot10^{-3} & -8.23\cdot10^{-3} & 4.716\cdot10^{-3} \\ 1.572\cdot10^{-3} & -8.645\cdot10^{-3} & 0 \end{bmatrix} \qquad GyroMLimits := \begin{bmatrix} 0.3 & 0.05 & 0.05 \\ 0.05 & 0.3 & 0.05 \\ 0.05 & 0.05 & 0.3 \end{bmatrix}$$

$$GyroBDiff = \begin{bmatrix} -2.408\cdot10^{-3} \\ 5.044\cdot10^{-3} \\ 3.777\cdot10^{-3} \end{bmatrix} \qquad GyroBLimits := \begin{bmatrix} 0.5 \\ 0.5 \\ 0.5 \end{bmatrix}$$

Acceptance

Accelerometer Alignment	AccMStatus = "OK"
Accelerometer Bias	AccBStatus = "OK"
Gyro Alignment	GyroMStatus = "OK"
Gyro Bias	GyroBStatus = "OK"

Other Outputs

The accuracy of the other measurements from the RT3000 change with the dynamic motion of the vehicle. The accuracy of these outputs are computed analytically using a Sensor Model in the Kalman filter and output as part of the Status Messages. During product verification we determined that it is possible to achieve the specifications in the User Manual based on the Sensor Model.

This Calibration Certificate ensures that the accuracy of the Accelerometers and Gyroscopes in the RT3000 is sufficient to meet the Sensor Model used in the RT3000. This, in turn, ensures that the Status Message outputs from the RT3000 are correct.

Results

The IMU complies with the acceptance conditions

Tested By:	Mike Redhead
Date:	26/02/08

The recommended recalibration period is two years.

RT-ANA Calibration Certificate

Equipment under Calibration

Model	RT-ANA
Serial Number	087
Software Dev ID	040505.14ax

Test Equipment Used

Procedure	14A0020A
Multimeter	Metrix Multimeter, Serial: 390025ZDX, 25/02/09 Cert No: E36164

Procedure

Each channel was calibrated at –9V and +9V then verified at –5V and +5V.

Measurements	All channels had 1mV error or less
Result	Pass

Config Version Valid: 60785645
CRC: BC3DF09F
CANBAUD 1000
CANID 0 610
CANID 1 611
CANID 2 612
CANID 3 613
DACCAL 0 2 61836
DACCAL 1 -7 61843
DACCAL 2 2 61850
DACCAL 3 1 61832
DACCAL 4 0 61839
DACCAL 5 1 61853
DACCAL 6 5 61829
DACCAL 7 -6 61812
DACCAL 8 5 61829
DACCAL 9 -1 61843
DACCAL 10 -7 61843
DACCAL 11 -6 61853
DACCAL 12 11 61829
DACCAL 13 -1 61836
DACCAL 14 -3 61839
DACCAL 15 -1 61843
FASTUPDATES OFF

Acceptance

The instrument complies with the acceptance conditions.

Tested by: Mike Redhead
Date: 04/03/08

The recommended recalibration period is 2 years after the calibration date.

Appendix B

DVD Disk

Two video cameras were used to provide a general view of the test sequence. Three high-speed video cameras and one high speed still camera was used to record the impact sequence, to show the failure mode and contact time between the impactor and approach lighting structure. The high-speed video cameras were capable of recording 2000 frames/second. The output from the videos and the still camera has been copied and assembled on a DVD disk for documentation purpose.

Figure 1: General test configuration

Figure 2: Typical attachment of the mast at the base

Figure 3: Rigid impactor

D106 pole

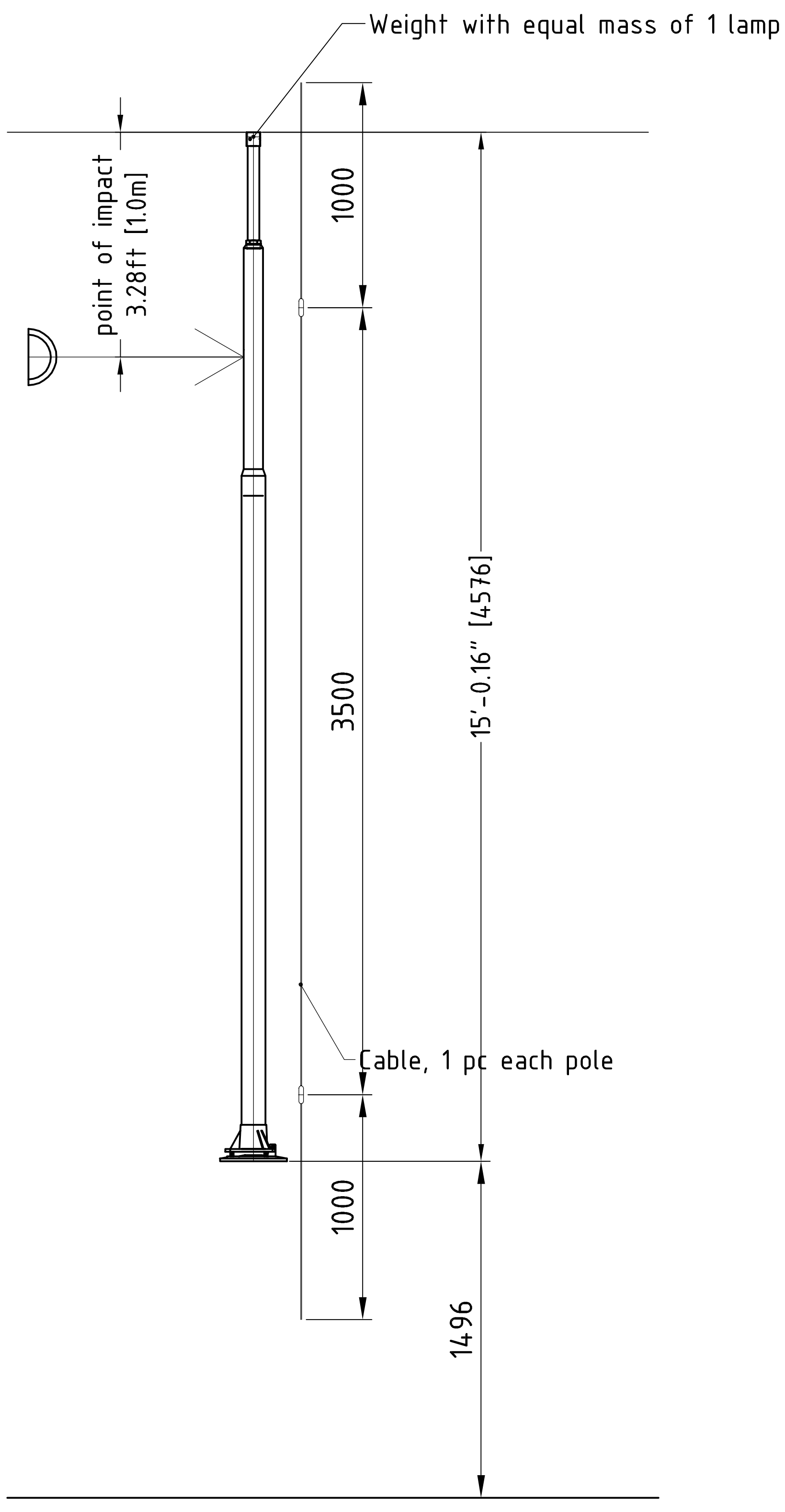

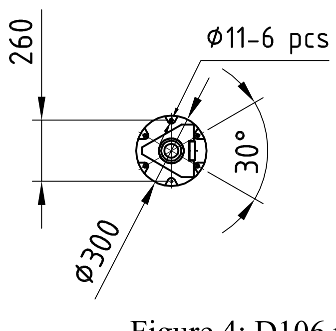

Figure 4: D106 pole structure

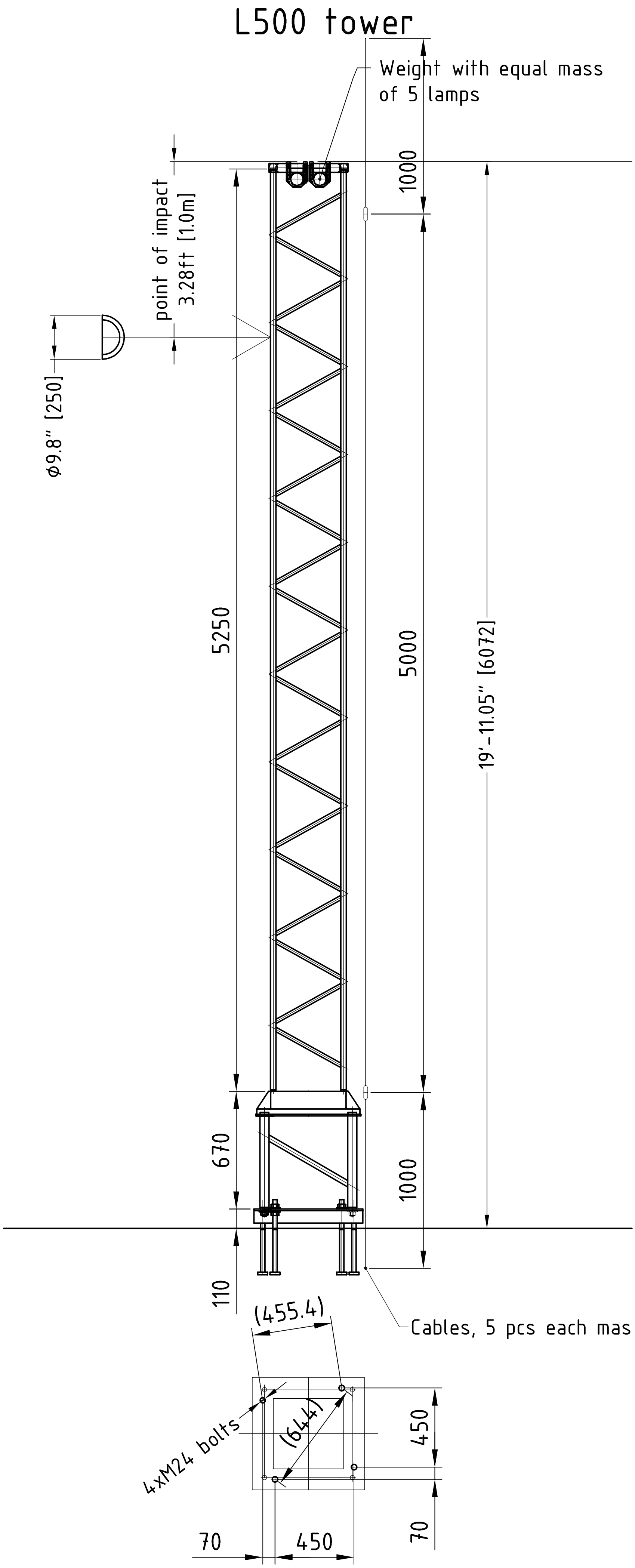

Figure 5: L500 lattice structure

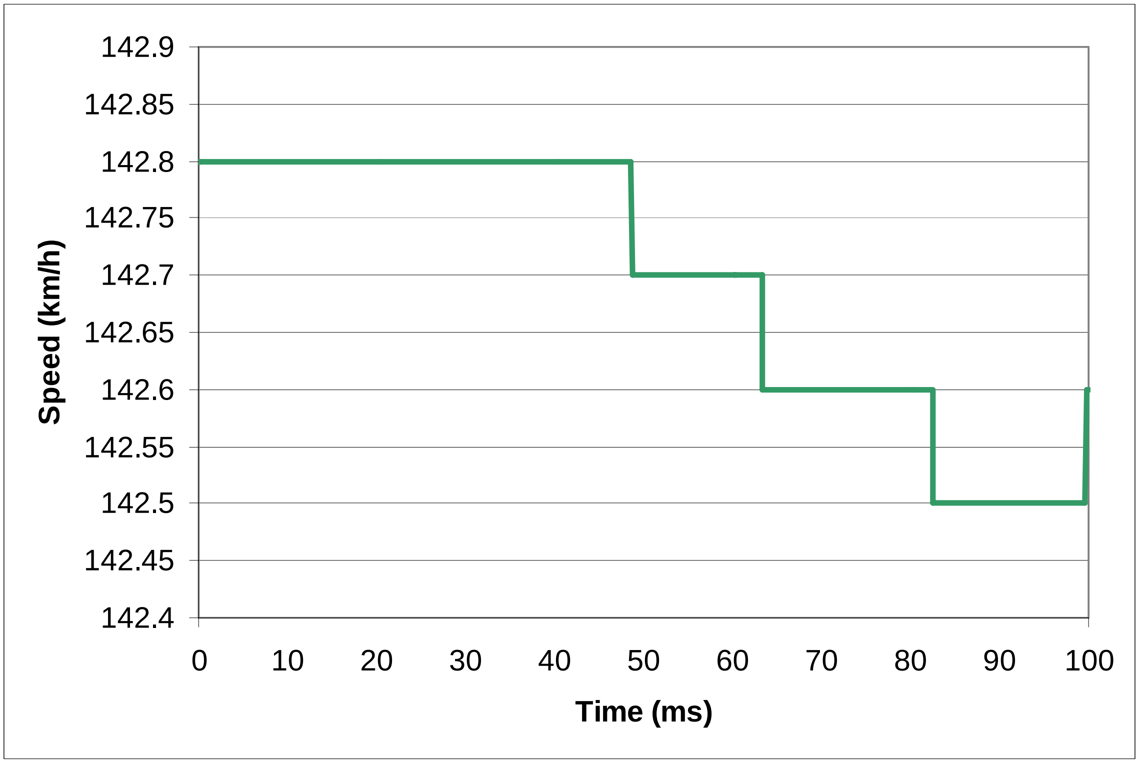

Figure 6: Speed over time from full-scale test of D106 pole

(a) 3 ms

(b) 40 ms

Figure 7: Impact events from full-scale test of D106 pole

(c)85 ms

Figure 7: Impact events from full-scale test of D106 pole

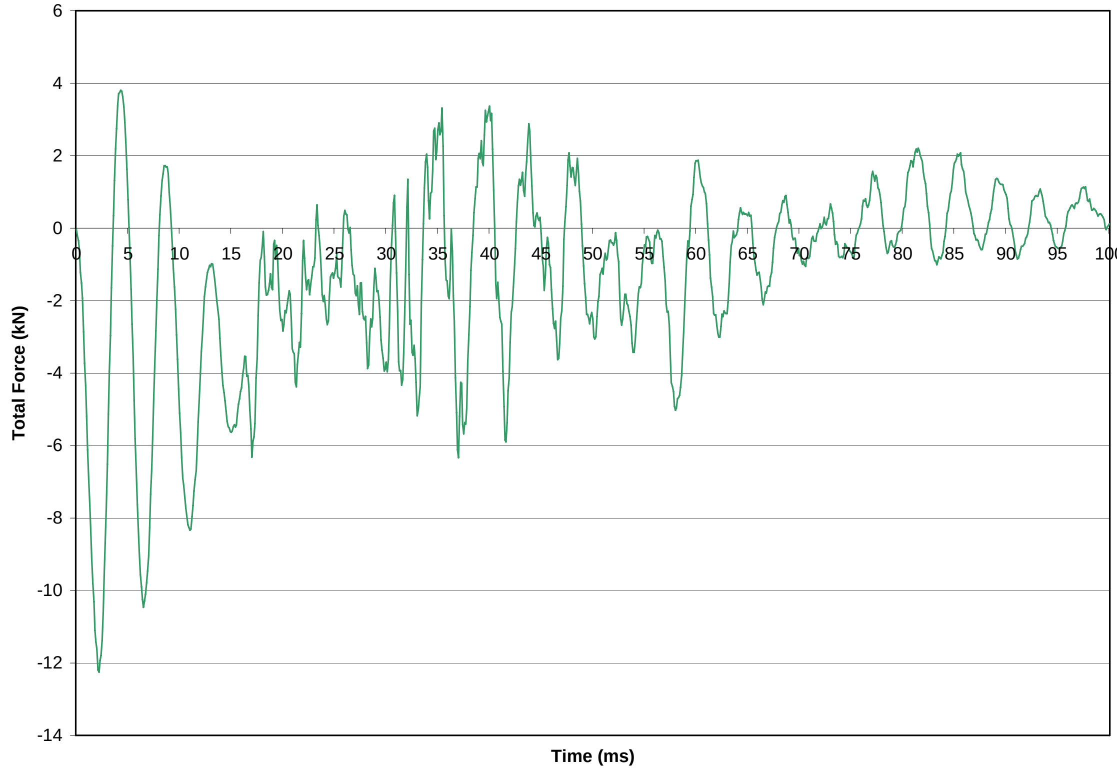

Figure 8: Impact force over time from full-scale test of D106 pole

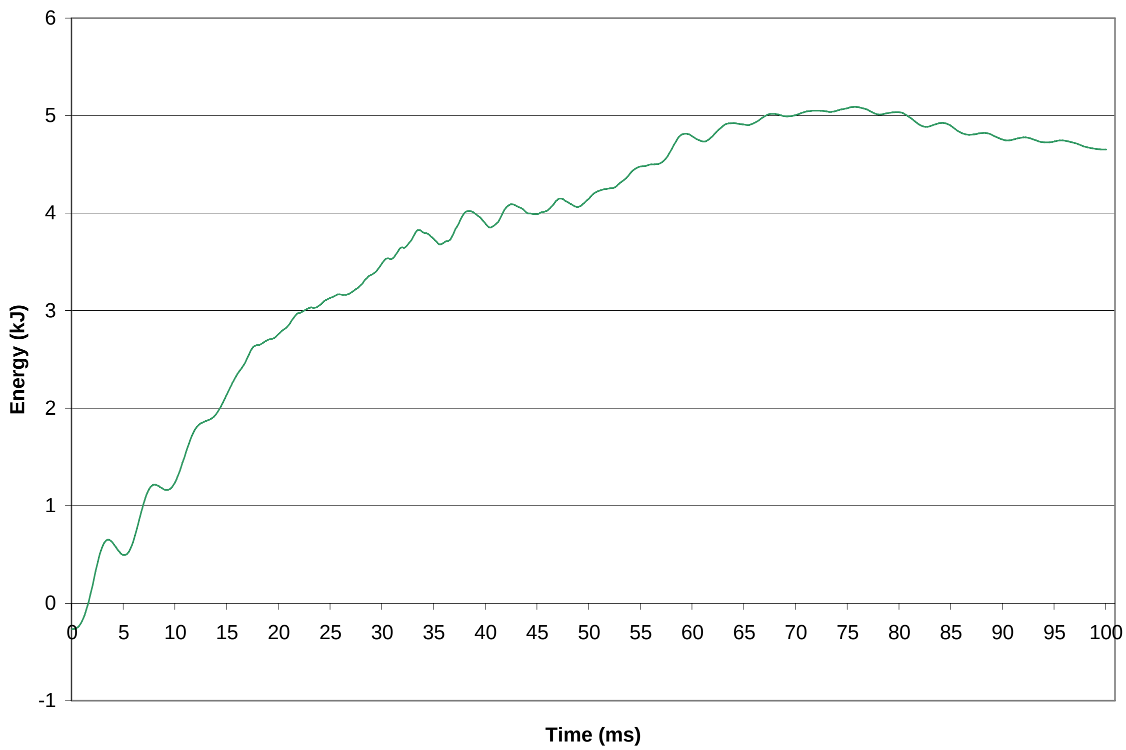

Figure 9: Energy absorption over time from full-scale test of D106 pole

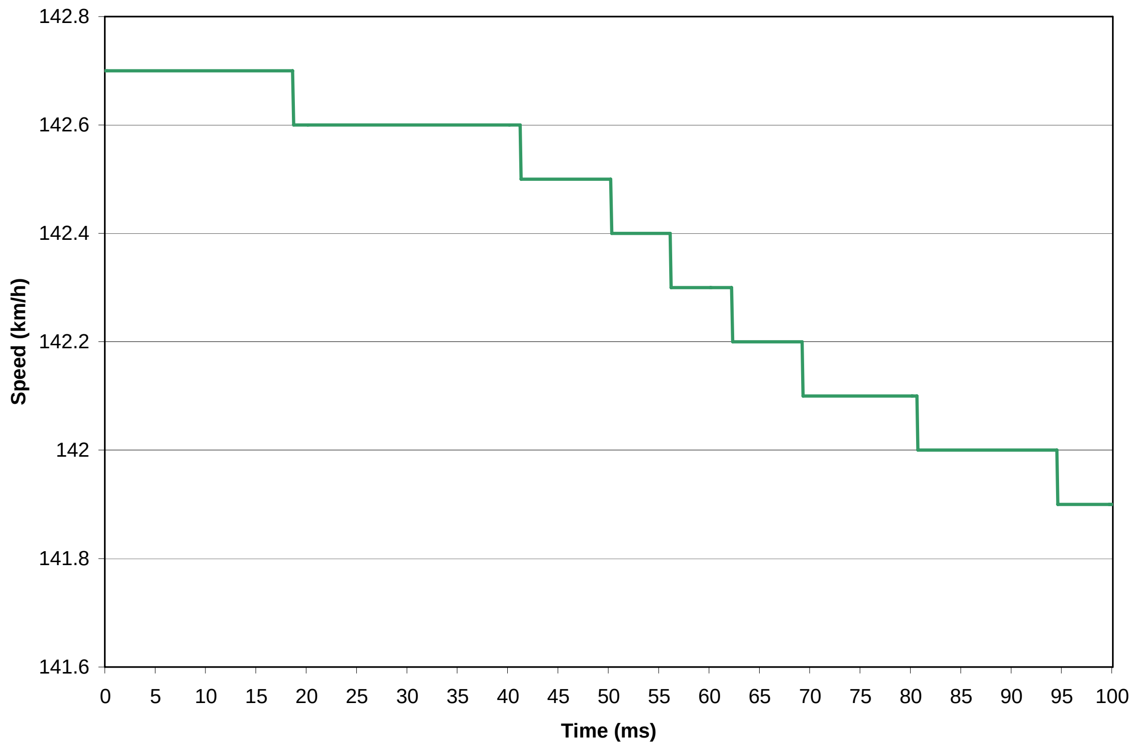

(a) Electrical cables run on impactor side

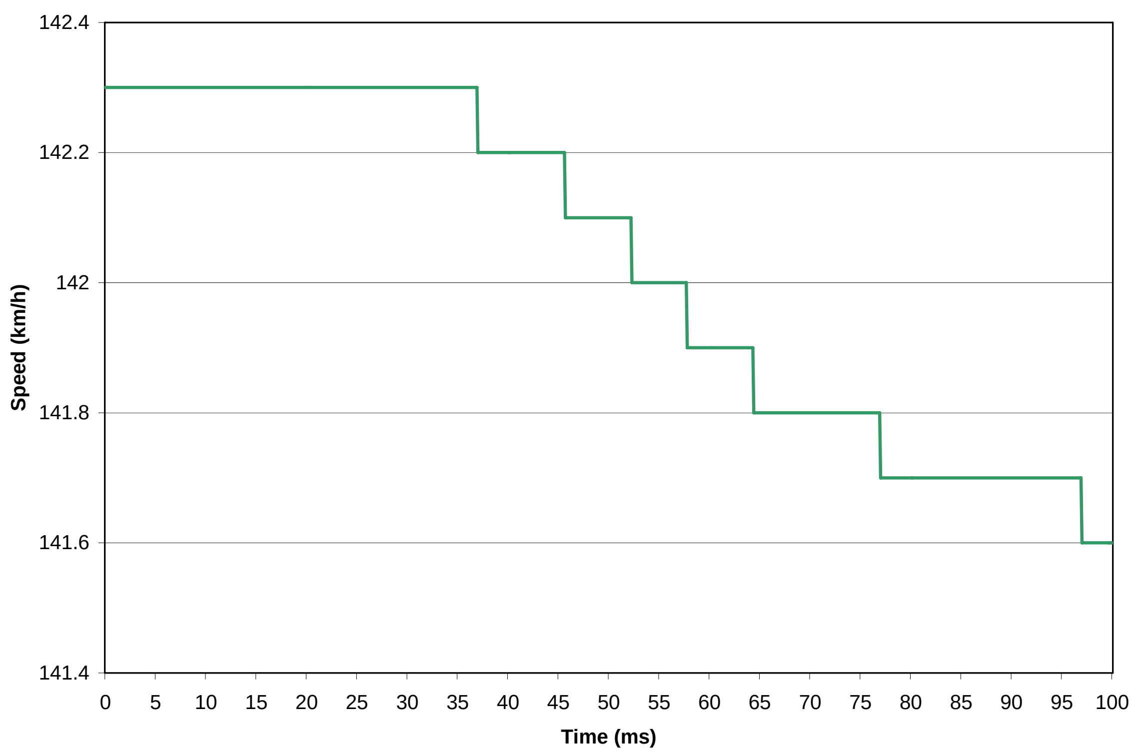

(b) Electrical cables run opposite to impactor side

Figure 10: Speed over time from full-scale test of L500 lattice tower

(a.1) After 2 ms

(a.2) After 25 ms

(a.3) After 65 ms
(a) Electrical cables run on impactor side

Figure 11: Impact events from full-scale test of L500 lattice tower

(b.1) After 2 ms

(b.2) After 25 ms

(b.3) After 65 ms

(b) Electrical cables run opposite to impactor side

Figure 11: Impact events from full-scale test of L500 lattice tower

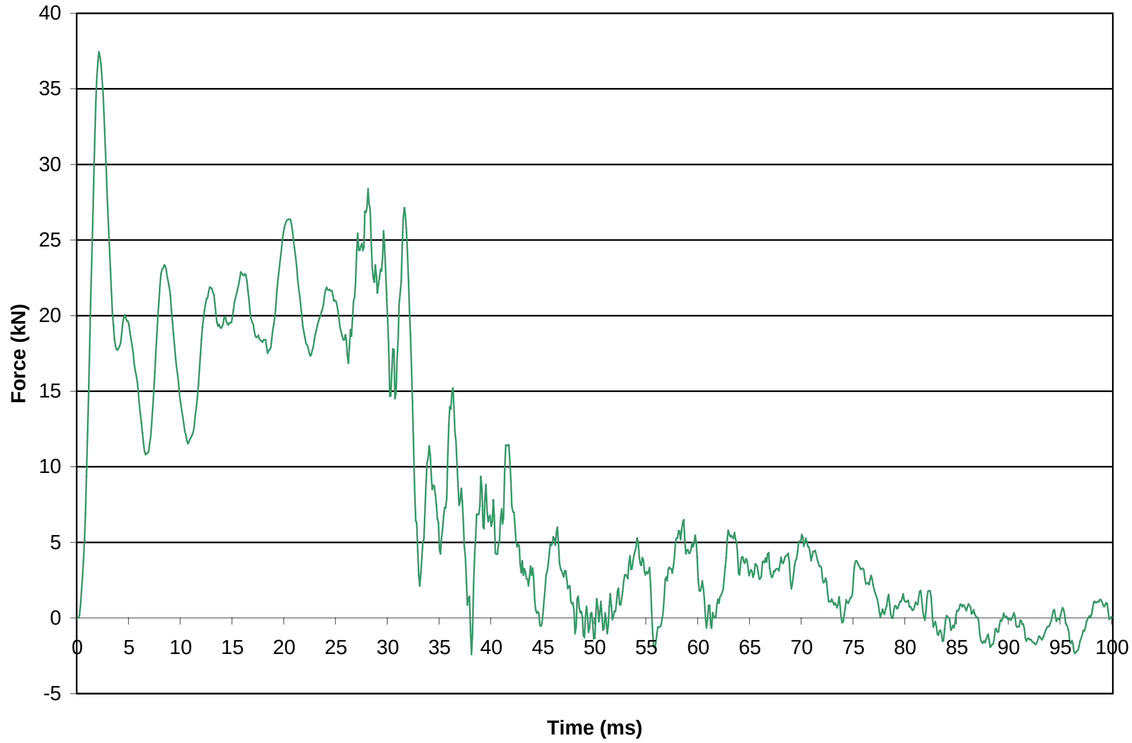

(a) Electrical cables run on impactor side

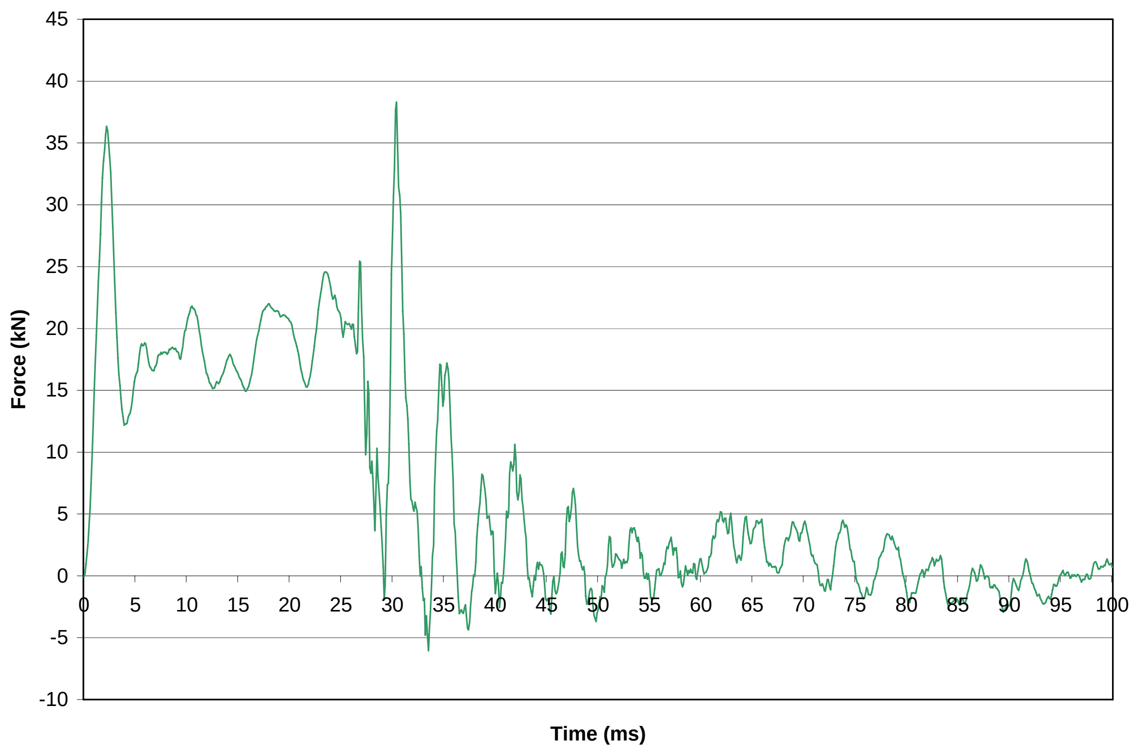

(b) Electrical cables run opposite to impactor side

Figure 12: Impact force over time from full-scale test of L500 lattice tower

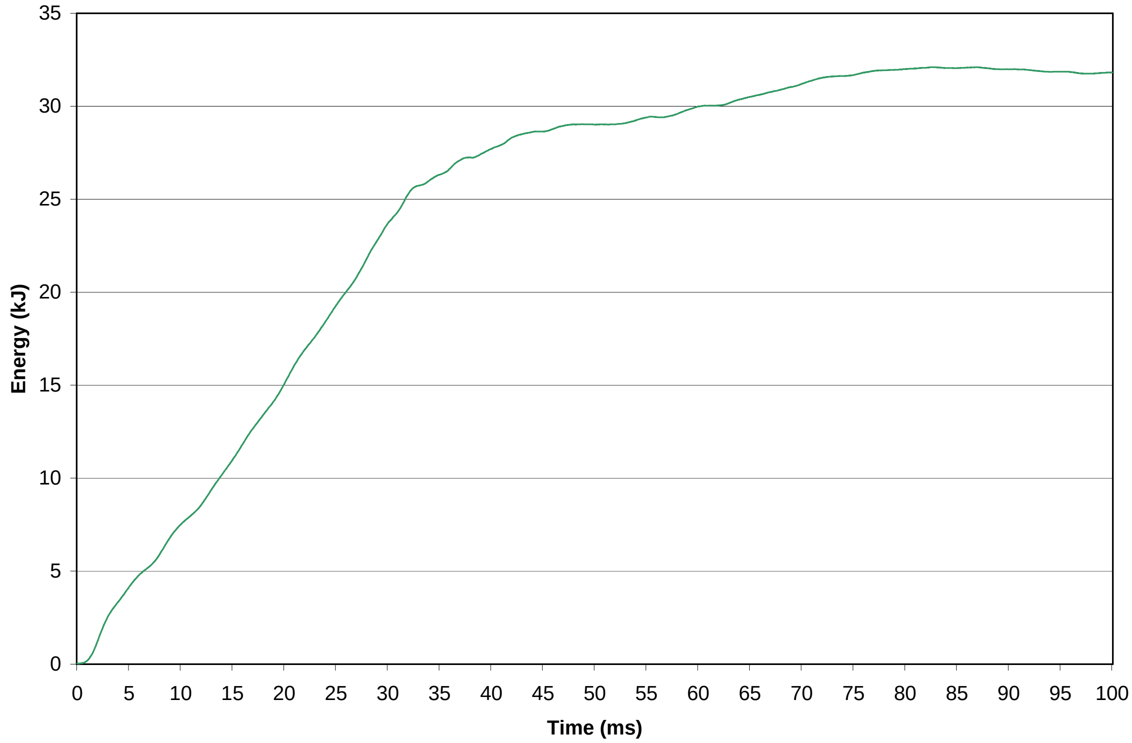

(a) Electrical cables run on impactor side

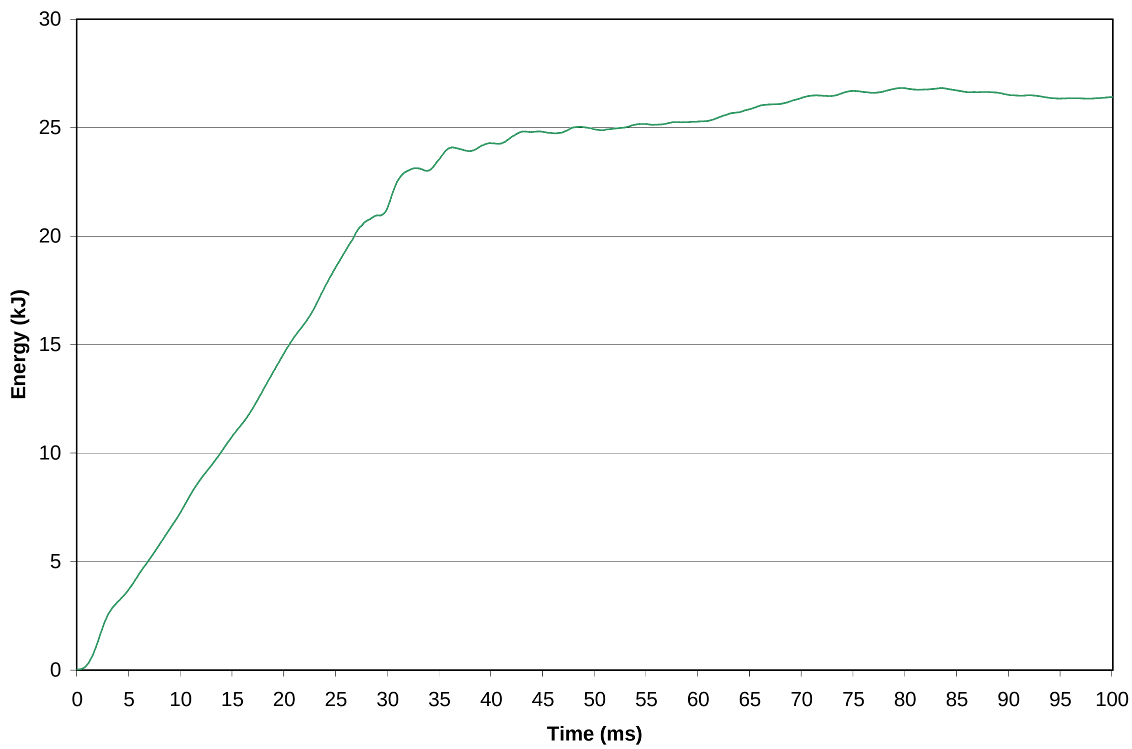

(b) Electrical cables run opposite to impactor side

Figure 13: Energy absorption over time from full-scale test of L500 lattice tower